

Structural and fracture analysis using EMI and FMI image Log in the carbonate Asmari reservoir (Oligo-Miocene), SW Iran

Ghasem Aghli^{1*}, Hashem Fardin², Ruhangiz Mohamadian², Ghasem Saedi²

¹Department Geology, Chamran, University, Ahvaz, Iran

²National South Iranian Oil Company (NISOC), Studies office, Ahvaz, Iran

*Corresponding author, e-mail: g-aghli@phdstu.scu.ac.ir

(received: 23/04/2014 ; accepted: 08/12/2014)

Abstract

Assessment of the reservoir structure and determination of the in situ stress direction are necessary in oil production optimization and field development. Today, the application of reservoir software and Image logs play a central role in resolving this problem. Electric and ultrasonic imaging tools record vast amounts of high-resolution data within the borehole wall. This enables the geoscientists to describe in detail the structural fracture networks very essential for stratigraphic and structural analysis and improved reservoir characterization. A Six Arm Electrical Borehole Imaging (EMI) tool has recently been developed. This tool represents further advancement in the evolution of electric borehole imaging. The electrode arrays mounted on six independent arms provide excellent pad contact and produce very high resolution images for stratigraphic and structural analysis. Furthermore, the results of this study indicate that EMI is a powerful technique for identifying the dominant porosity and defining the relationship between fractures and permeability. In this study, data from two wells (well No.3 with FMI and well No.6 EMI image log) were utilized. The results of the Velocity Deviation Log and images indicate that the production in the Asmari reservoir of this field is a combination of fractures and rock matrix. Besides, the fractures and porous zones have effectively impacted the reservoir rock properties so that two general patterns of tectonic fractures associated with longitudinal and diagonal wrinkling can be identified. Longitudinal patterns are the dominant ones and often form the open fractures. They are mainly oriented in the N45-90W direction and are chiefly observed in the upper Asmari zones. Induced fractures and breakouts have been observed in the two wells, indicating a maximum horizontal stress orientation of 65°N in well No.6 and 295°N in well No.3. The stress direction in the western section of this oil field is therefore different from the eastern one and does not follow the general Zagros trend.

Keywords: Balarud Fault, Fractures, EMI, FMI Image Logs.

Introduction

Fractures play a vital role in the production and migration of oil in the Zagros basin, which is a world renowned feature of the Iranian carbonate reservoirs (Roehl, 1985). Several studies have been published on fractures in this region (e.g., McQuillan, 1973, 1974; Gholipour, 1998; Rezaei & Nogole-Sadat, 2004; Ahmadhadi *et al.*, 2007, 2008; Khoshbakht *et al.*, 2009). Based on the works of Ahmadhadi *et al.*, (2007, 2008) the regional fractures in the Asmari Formation are mostly sub-vertical and interpreted to have been initiated before the main Mio-Pliocene folding phase of the sedimentary cover. Hence, the fracturing observed in the Asmari Formation is interpreted as a consequence of the reactivation of the deep basement faults associated with the continental collision of the Arabian plate with Central Iranian plate (Alavi, 2007).

The carbonate reservoir fractures are important as they have effectively influenced the reservoir rock properties that deal with porosity and permeability; also, the relationship between the

present day stress field and natural fractures can have significant implications for subsurface fluid flow (Serra, 1989). The presence of fractures -even very fine ones- has a considerable impact on the permeability (Rezaei & Chehrizi, 2005) and knowledge about them and their scattered patterns are helping in determination of the best location for drilling and maximum exploration (Serra & Serra, 2004). Furthermore, it is the knowledge of stress orientations at smaller basin and field scales that is of critical importance for petroleum applications such as wellbore stability and hydraulic fracture stimulation (Bell, 1996; Tingay *et al.*, 2005). In the analysis of fractures on the carbonate reservoirs a large amount of data is used from various sources such as structural data, drilling data, petrophysical logs, cores data, production wells data and dynamic wells data (Tampson, 2000). The best method for fracture analysis is image logs. They cut costs by reducing the coring intervals and perforate zone determination (Schlumberger, 2005). Such tools normally provide the best high-resolution borehole images in the conductive (water-based) muds.

Examples are the Electrical MicroImager (EMI) and Fullbore Formation MicroImager (FMI) (Halliburton, 1996). The drilling-induced fractures, breakouts, and petal-centerline fractures that are assumed to form just ahead of the drill bit will provide additional constraints on the orientation of the minimum horizontal regional stress (Rajabi *et al.*, 2010; XinNie *et al.*, 2013). In between determination of the in situ stress is very important in the drilling and perforating stages, because any error will cause the wellbore wall to collapse.

Geological setting

The area under study is located in the North Dezful Embayment (SW Iran), which is part of the Zagros fold-and-thrust belt (McQuarrie, 1974; Alavi, 2007, 2004). The Zagros mountain range is a collisional belt between the Iranian block (belonging to Eurasia) and the Arabian plate, whose convergence commenced at the beginning of the Late Cretaceous period (Ricou, 1974; Berberian & King, 1981) and accelerated during the Late Miocene and Pliocene (Stocklin, 1968). The convergence is still active today, in a NNE–SSW direction (DeMets *et al.*, 2010). The Asmari Formation (Oligo-Miocene) is composed of light gray (locally buff to white) shallow-marine Hippurite-bearing limestone (grainstone, pelletal packstone, dark bioclastic wackestone) with intercalations of black fissile

shale and broken by several intraformational unconformities (Alavi, 2004). The field under study is a fault- bend fold that has strictly been influenced by the Balarud shear zone (Sahabi, 2010). The existence of the Balarud reverse fault and three strike-slip faults at the southern edge has caused great difficulty in structural analyses (Fig. 1a). Based on seismic mapping, this anticline is more than 17 km long and 8/7 km wide. The southwest edge of the anticline is more inclined towards the edge of the North East along the axis of the building it is close to 118 degrees azimuth, in the southeast- northwest direction. The anticlines and reverse faults in the shear zone located approximately 1000 m to the south are trusted. Some areas show an overturned limb (Fig. 1b) and the stratigraphic column is shown in Figure 1c.

Borehole Imaging Tools and their application in the geology reservoirs

Imaging tools can be used in a wide variety of geological and drilling environments, providing borehole images of rock, from the karstic carbonates to soft thinly laminated sand/shale sequences. High resolution and often almost complete borehole coverage images are interpreted at an interactive graphic workstation.

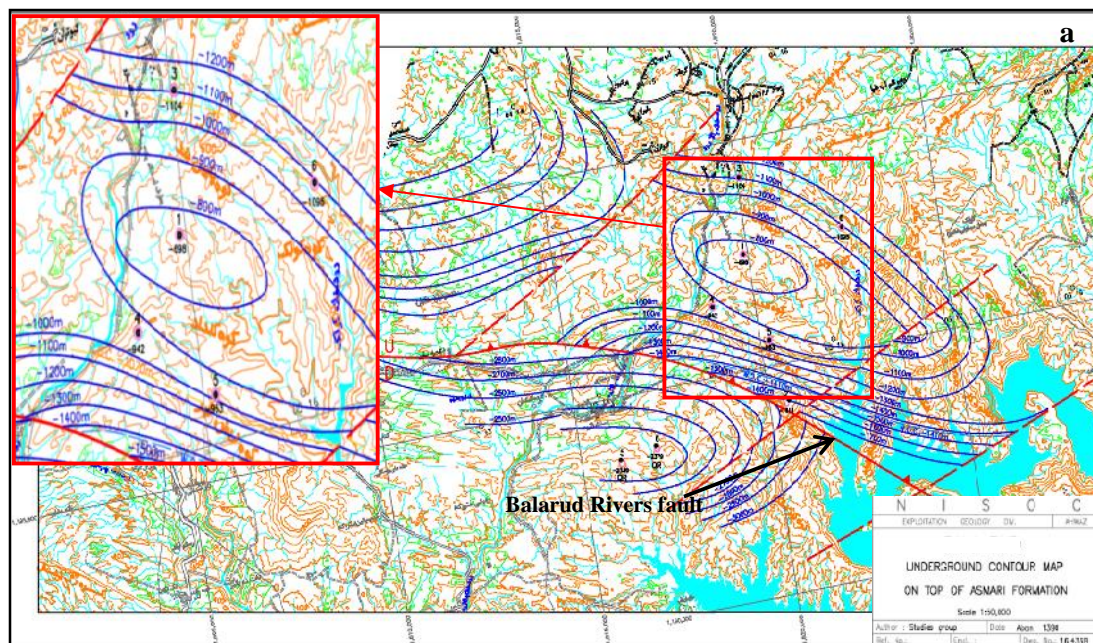


Figure 1-a. UGC map the Studied Field and wells location, provided by NISOC (2011)

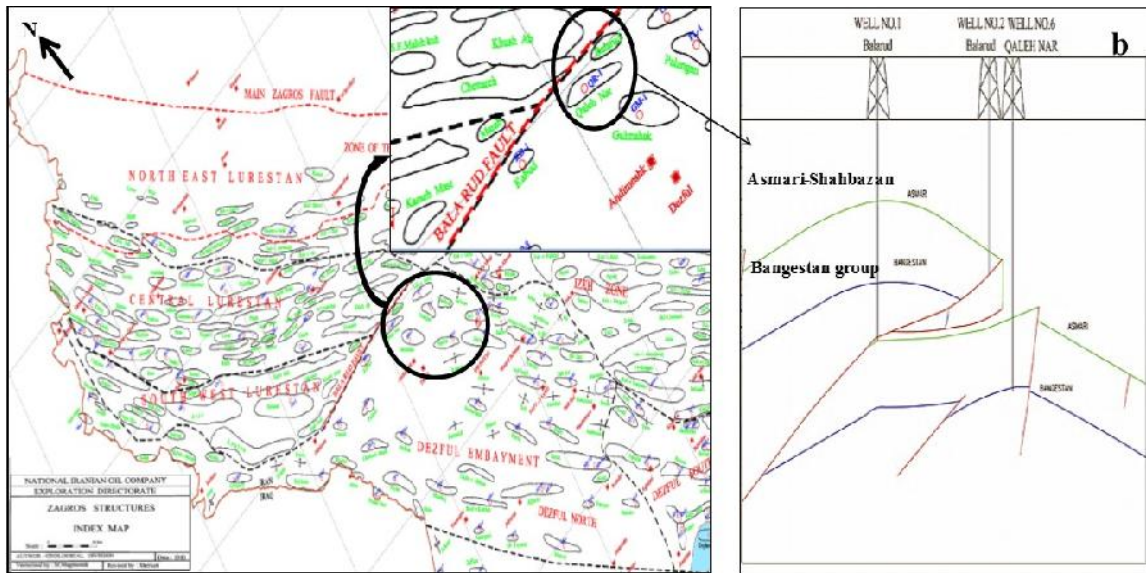


Figure 1-b. Position Balarud Trust belt and Balarud oil fields in Dezful Embayment and cross section of Balarud-Ghalehnar oil fields and studied Formations

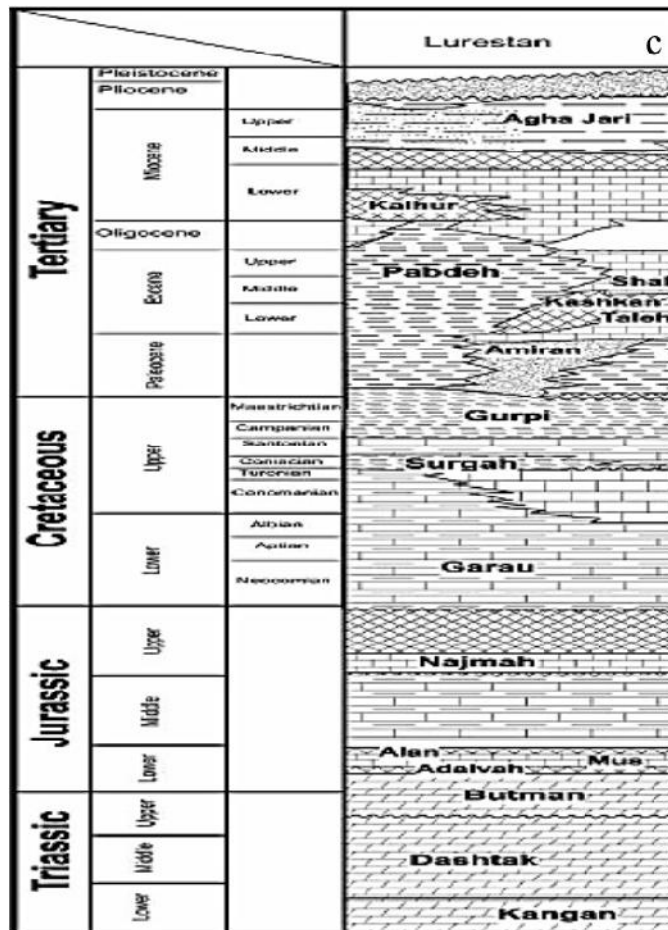


Figure 1-c. stratigraphic column of the study area (Gachsaran and Aghajary formations are surface outcrops) (Sepehr & Cosegrov, 2004)

When the image is “unrolled” and displayed from 0° to 360°, linear features intersecting the borehole appear as sinusoids (Rider, 1996). Assuming that the images are properly oriented to the geographic north, the peaks and troughs of the sinusoids can be related to the dip and azimuth of the associated feature, respectively. This consequently provides fundamental information regarding the formation encountered that other petrophysical logs are unable to provide. Bedding, fracture features, faults, stratigraphic features, and many other characteristics can often be manually or (semi-) automatically identified and quantified (Ye & Rabiller, 1998).

Besides identifying the fractures and faults, borehole imaging tools are routinely used in the support of detailed core analysis for a variety of other applications such as sequence stratigraphy, facies reconstruction, and diagenetic analysis. In general, the electrical images appear to be sensitive

to variations in mineralogy, porosity, and fluid content that highlight both natural fractures and rock fabric. The acoustic image logs reveal a similar natural fracture population, not the rock fabric, due to their lower resolution. However, due to their full coverage, the acoustic images can reveal drilling-induced borehole wall tensile fractures, breakouts and petal- centerline fractures (Tingay *et al.*, 2008). The FMI tools have an azimuthal resolution of 192° capable of radial micro-resistivity measurements (vertical resolution: 0.2”, vertical sampling: 0.1”, depth of investigation: 30”; (Schlumberger, 1994). The EMI Electrode arrays are mounted on six independent arms providing excellent pad contact. This produces very high resolution images for stratigraphic and structural analysis (Halliburton, 1996). These two tools cannot be used in the oil based mud where OBMI and UBI are applied (Table 1).

Table1. The comparison between imaging tools (Tokhmchi, 2009)

Manufacturing company	Depth investigation (mm)	Max logging speed (m/hour)	Number of electrodes on each flap	Number of flaps	Borehole coverage in 8 inch	Resolution		Tool name	Type of mud	Method imaging
						V	H			
Schlumberger	15-50	500	16	4	40	5		FMS	Conductive	Electrical
Schlumberger	15-50	565	34	8	800	5	7.5	FMI		
Schlumberger	750	1125	12	-----	100	200	5	ARI		
Halliburton	750	584	25	6	80	5	30	EMI		
Baker Atlas	-----	-----	24	6	65	7.5	5	STARE		
Schlumberger	9	1125	10	4	32	30	5	OBMI		
Baker Atlas	-----	-----	10	6	-----	-----	30	Earth Imager	Non conductive	
Schlumberger	-----	135	-----	-----	100	10		UBI	Con & non con	Sonic
Baker Atlas	-----	-----	-----	-----	100	-----		CBIL		
Halliburton	-----	360	-----	-----	100	75		CAST		
Schlumberger	-----	-----	-----	-----	10	11		BHTV	Con & non con	Borehole televiewer

Electrical Micro Imager (EMI)

The Electrical Micro Imaging (EMI) tool is a new logging service that provides core-like images of the borehole wall by measuring and mapping the formation micro- conductivity with pad-mounted button electrodes. The superior 3D and 2D images produced by the EMI are possible as the design uses six independent articulating arms to maintain consistent pad contact against the borehole wall (Halliburton, 1996). Formation images are achieved using the 150 pad-mounted sensors distributed at 25 per pad, on each of the six pads, resulting in a measurement (Fig. 2). The current in each button is recorded as a curve, sampled at 0.1 inch (0.25 centimeters), or 120 samples per foot (Fig. 3). The

curves reflect the relative micro-conductivity variations within the formation. These current variations are converted to synthetic color or gray-scaled images. The light colors represent low micro conductivity, while the dark colors reflect high micro- conductivity zones (Serra & Serra, 2004). Centralization above and below the EMI Mandrel optimizes the distribution of the six pads across the circumference of the borehole, especially in the horizontal and highly deviated wells. A full navigation package, including three orthogonal fluxgate accelerometers and three orthogonal magnetometers, is included in the EMI tool to provide accurate information on the tool position, motion, direction, and orientation within the

borehole. The acceleration in the direction of the tool body axis is used to calculate a speed-corrected image. The tool can be run either in dip mode and /or image mode, and all button resistivity data are recorded at a maximum logging speed of 1800 ft/hr. In the dip mode, the tool mimics the SED and sends only the center button resistivity data up the hole which enables a maximum recommended logging speed of 3600 ft/hr. The electrical tools are the best tools to record this activity between (FMI) with azimuthal resolution vs 192 and are capable of radial microresistivity measurements (vertical resolution 0.2", vertical sampling: 0.1", depth of investigation: 30"; Schlumberger, Ltd., 1994). The EMI electrode arrays are mounted on six independent arms providing excellent pad contact, resulting in very high resolution images for stratigraphic and structural analysis (Halliburton, 1996). Both these tools lack the capacity for use in the oil based mud and therefore the two tools OBMI and UBI were constructed.

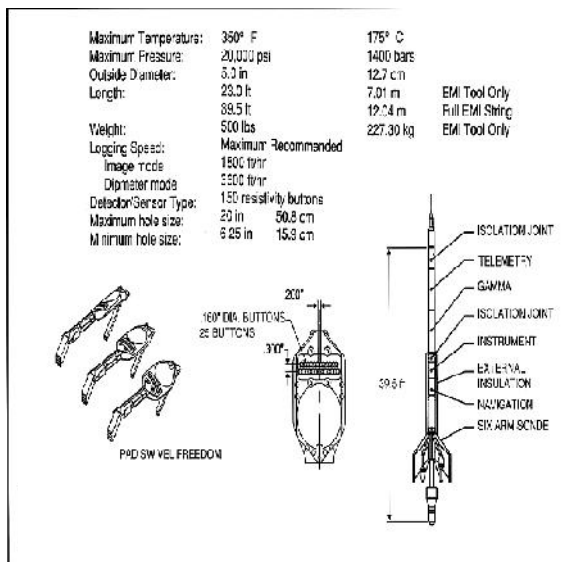


Figure 2. display of EMI tool Characteristics (Halliburton, 1996)

Why use the EMI Service?

This tool has features that differentiate it from the other tools. For example one of the important EMI features is the presence of six articulating pads, each mounted on an independent arm, facilitating improved electrode-to formation contact. The independent arm action indicates that variable pad pressure is maintained against the borehole wall during logging. The Electrical Micro Imaging tool

has scanning electrode arrays on each of its six independent arms. Superior imaging is produced through consistent pad contact with the borehole wall which provides accurate and sharp images. Another important characteristic of the EMI is the great depth of investigation, almost 20 times more than that of the FMI tool (Table 1). This ability is vital for the study of vuggy reservoirs, particularly in measuring their density and their connectivity (Aghli, 2013).

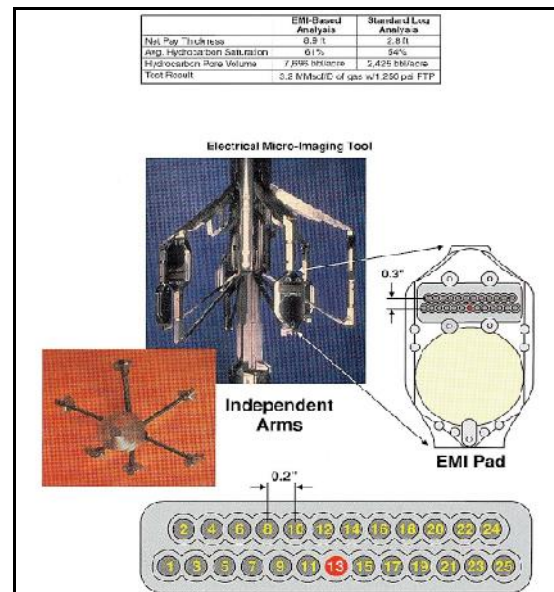


Figure 3. the electrical Micro-Imaging tool uses pad-mounted electrodes to make high-definition resistivity measurements (Serra, & Serra, 2004)

EMI reduces expenditure by reducing the coring intervals and perforate zone determination. Besides providing better data to boost production, EMI helps cut costs by improving the drilling and completion efficiencies. In many cases, the conventional coring programs can be reduced or even eliminated. The well completions in the multi-layered, thinly bedded or fractured reservoirs can be optimized. Image analysis and enhancement techniques are available for precise identification of formation reservoir characteristics and include the following features (Fig. 4, Halliburton, 1996):

- Detailed stratigraphic and sedimentological analysis
- Thin bed delineation
- Potential secondary porosity identification
- Fracture analysis
- Quantitative high-resolution resistivity for

- improved net pay estimation
- Fault mapping

- General structural analysis.

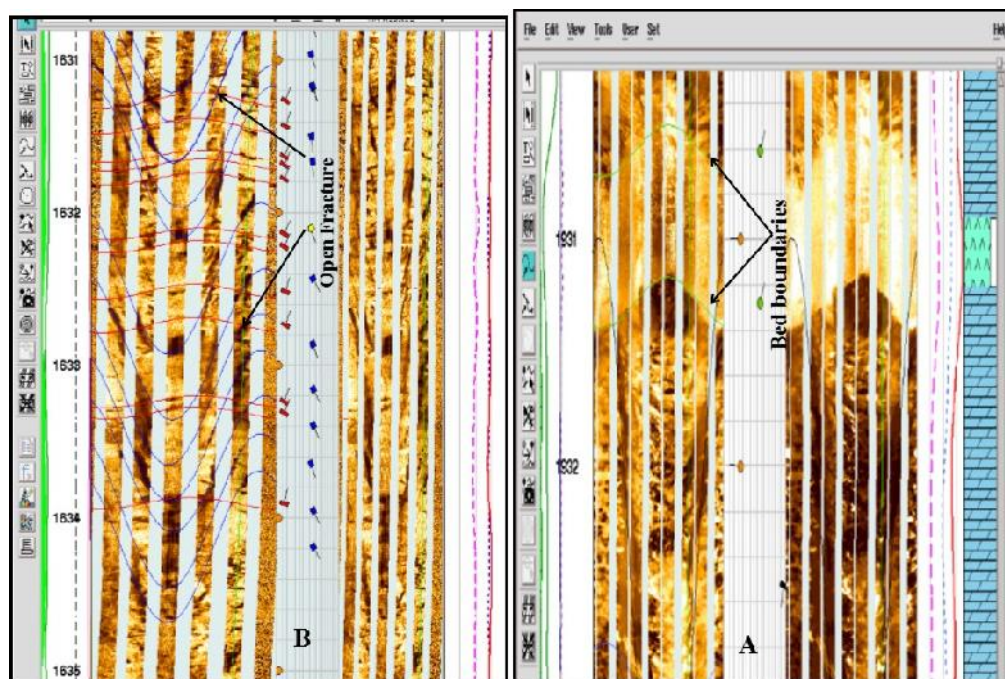


Figure 4. Fractures displayed on image log. (A) EMI image log and (B) FMI image log

Methods

Images were produced at the well sites. Detailed post-acquisition analysis of the image data was done with high-performance interview analysis software. Image analysis and enhancement techniques were available to identify precisely the characteristics of the formation reservoir (Fig. 4), including detailed stratigraphic and sedimentological analysis, thin bed delineation, potential secondary porosity identification, fracture analysis and fault mapping (Schlumberger, 2003).

The main purpose of this study was to systematically study the Asmari reservoir fracturing and bedding, their direction and type, methods to extend the fracture in the reservoir, their generation mechanisms, determination of the *in situ* stress direction and determination of the permeability zone using the Geoframe 4.5 software.

Results and Discussion

After the analysis of the image logs in the two wells Nos. 3 and 6 (Fig. 1), several features such as fractures, beddings, induced fractures, borehole breakouts and stylolites were identified. To facilitate the analysis, software showed the data in stereonets, rose diagrams and histograms. Further

on, the results of each well will follow as separate sections, along with the EMI ability in well No. 6.

Well No. 6 (EMI)

Structural analysis and open/close fractures density

The key to producing fractured reservoirs economically is to obtain sufficient information to estimate the recoverable reserves and predict an optimum well location. Borehole imaging is an excellent method for evaluating fractured reservoirs. Along with providing better data to boost production, the EMI helps cut costs by enhancing the drilling and completion efficiencies. In many cases, conventional coring programs can be reduced or eliminated. Also, the well completions in multi-layered, thinly bedded or fractured reservoirs can be optimized, with improved electrode-to-formation contact. The EMI is based on Halliburton's award-winning Six-Arm Dipmeter (SED) technology (Halliburton, 1996). In well No. 6 (Eastern Cape of North Flank) in the Asmari reservoir, which is a heterogeneous one, there are 485 open/closed fractures. Their dip inclination varies from 20° to 50°, with their strike dominantly in the N80W and their azimuth varying

from 190° to 200° from the north (Fig. 5). Both low and high confidence resistive fractures show large scatter in their dip azimuth and strike. In this well the fractures are classified into two groups. One set of fractures shown by (E) have the same as bedding strike and are classified as the longitudinal set.

Their strikes in this well are N80W. The other fracture set shown by (F) reveal oblique strike relative to the bedding strike and are, therefore, considered as oblique fractures. Their strikes are N75E (Fig. 5).

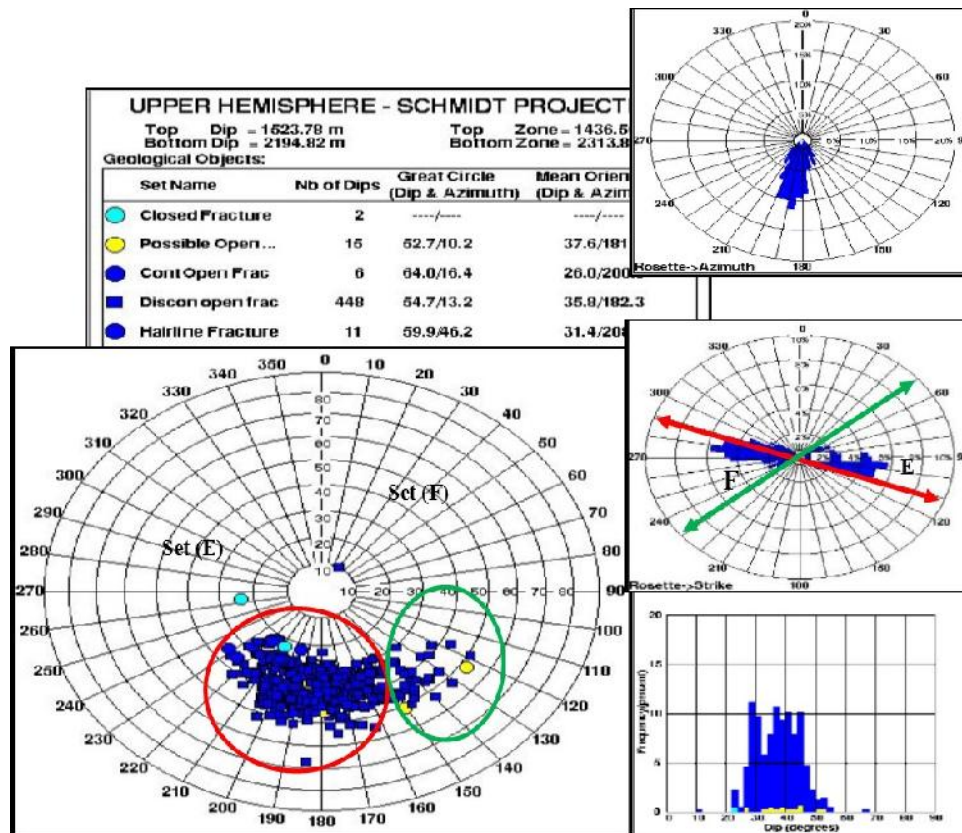


Figure 5. Stereonet rose diagram and histogram of fractures in the well 6 indicated on EMI image log

Vugs

Another common type of secondary porosity found in carbonate reservoirs are vugs. Diagenetic in nature, vugs are formed when the migrating formation water dissolves the unstable material in the surrounding rock or by sub aerial exposure of the rock. Although difficult to analyze with the conventional logging tools (Serra & Serra, 2004), the EMI is able to image the reservoirs containing the secondary porosity, enabling the analyst to determine the density and connectivity of the vugs. Figure 6 compares a vuggy carbonate Velocity-Deviation Log (VDL) and EMI image. In the EMI image, the filled vugs appear as light colored objects ringed by darker colored conductive material, while the open (fluid filled) vugs appear darker than the surrounding matrix and the VDL

logs indicate readings above +500 in the vuggy zone and <-500 in the fracture zone and between +500 until -500 if the rock matrix has an important role in reservoir porosity (Anselmetti, F.S. and Eberli G.P., 1999). In this field the production in the Asmari reservoir is a combination of fractures and rock matrix (Fig. 6).

Identification and Characterization of Sedimentary Features:

Evaluating thin-bed formations using a high-resolution resistivity curve will reduce the risk of miscalculating the hydrocarbon reserves. The EMI can image bed thicknesses from a fraction of an inch to several feet. This facilitates easy identification of the sand/ shale facies in the formation, and permits very accurate calculations

ofsand thickness counts. Laminated reservoir sections may not be detected if conventional resistivity tools are used. The EMI images are sufficiently detailed to enable the description of many sedimentary features including bed boundaries, internal bed characteristics, textural changes, primary and secondary sedimentary structures, and thinly laminated

sand/shale/carbonate sequences. Using these features, it is possible to identify the depositional environments and determine the paleocurrent direction. Figure 7 shows an example from the upper section of the fluvial channel sand. Recognizable features include a well-defined bed boundary, contorted bedding, shale drape, and cross bedding (Halliburton, 1996).

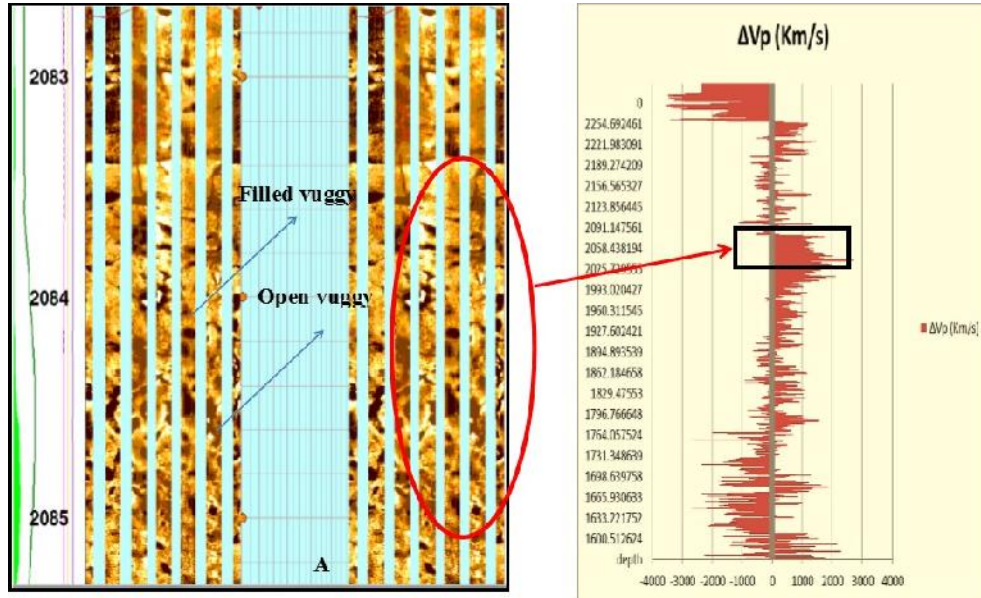


Figure 6. Display vugs (A) EMI image log as is evident can determine the density and connectivity of the vugs and (B) Velocity-Deviation Log indicate Readings above +500 in the vuggy zone

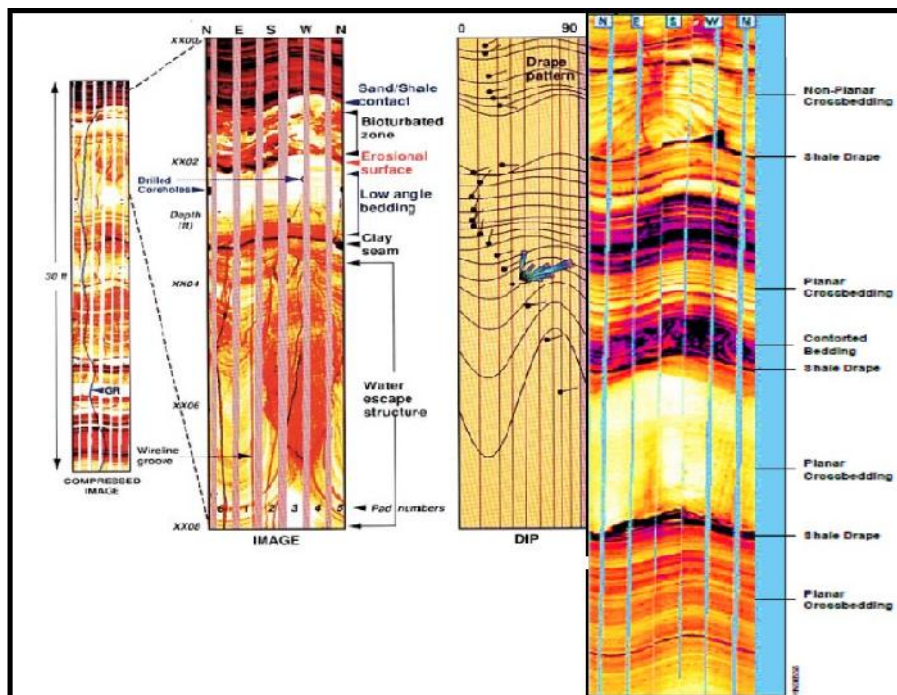


Figure 7. Recognizable features in a fluvial sandstone log section (Halliburton, 1996)

Structural Dip description to this well:

The accuracy of the structural dip is dependent on the planarity and sharpness of bed boundaries; therefore, the layer/ bed boundaries were classified under High Confidence and Low Confidence categories as far as their dips are concerned. There are 98 low confidence (LC) beddings and 3 high confidence (HC) beddings recognized over the entire interval. Both LC and HC beddings were used to determine the structural dip. However,

significant variations in the bedding dip were present which made it difficult to identify the major structural dip.

However, the structural dip was deduced to be 8 degrees toward N55E and strike N30W. It is notable that the long distances between this well and the strike-slip faults and Balarud fault, bedding are more regular and their dips are less than that of the other wells (Fig. 8)

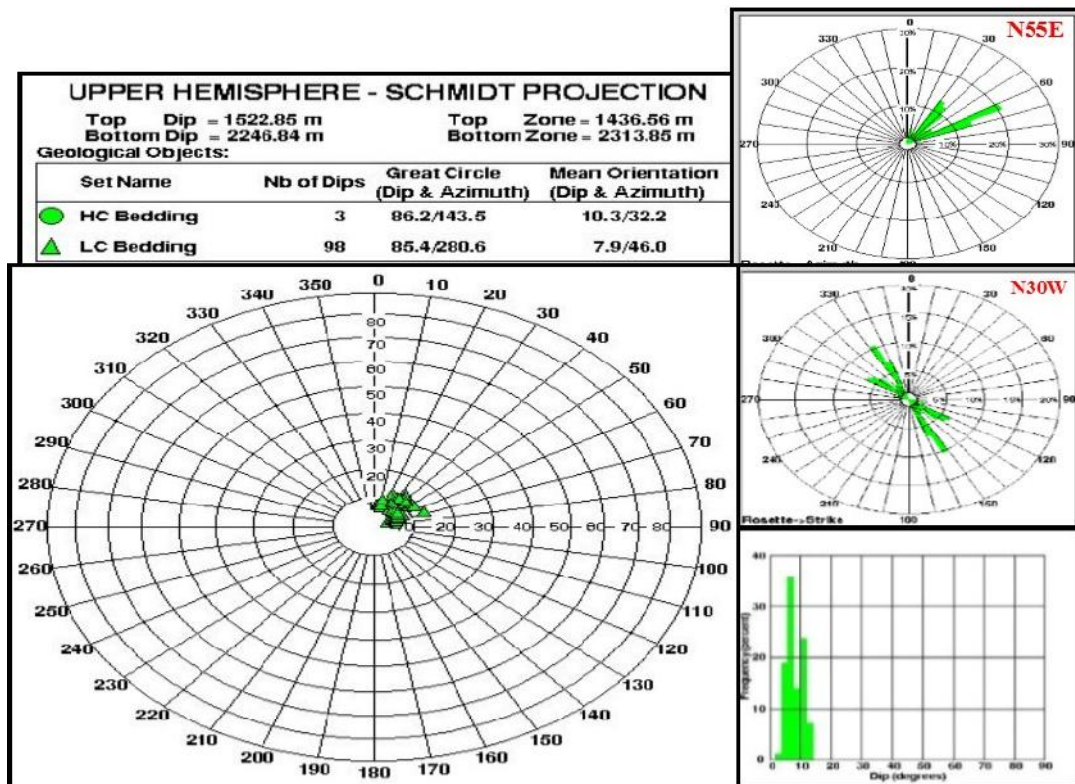


Figure 8. Stereonet, rose diagram and histogram of bedding in the well 6

Well No. 3 (FMI)*Structural analysis and open/close fractures density*

In well No. 3 (Western Cape of North Flank) in the Asmari reservoir, which is a heterogeneous reservoir, 665 open fractures are present. Their dip inclination varied from 30° to 80°, but their strike was dominantly N-E and their azimuth varied from 180° to 200° from the north (Fig. 9). Both low and high confidence resistive fractures showed large scatter in their dip azimuth and strike. In this well, the fracture type can be estimated as fractures related to folding which can be classified under two groups, based on the relative fracture strike and

bedding strike (oblique and longitudinal sets). One set of fractures shown by (A) have the same strike as the bedding strike; hence the term longitudinal set. Strikes in this set are almost N-W. The other set of fractures shown by (B) have oblique strike into bedding strike; hence, they are considered oblique fractures. Strikes in this set are N70E (Fig. 9). It is notable that the high density fractures in well No. 3 are related to the axis re-circulation by the strike-slip fault near it (Aghli, 2013).

Structural Dip description

Layer/bed boundaries in carbonate sequences are not always sharp and planar, due to diagenetic

processes, to be used for structural dip determination. In the FMI loglines, marking abrupt and relatively high resistivity contrasts that cross all the images is necessary to identify the bed boundaries (Darlyng, 2005; Saedi, 2010). These lines are easily correlated from pad to pad and are visible on the static images. Their lines correspond to the surface or boundaries separating two beds of different lithology (Serra, 1989). Two types are observed: The first set, in which the dips correspond to sharp and well planar bed / layer boundaries are categorized as High Confidence (HC) whereas in the second set the dips corresponding to vague and uneven bed / layer surfaces are categorized as Low Confidence (LC). In this well, axis re-circulation is the cause of bedding shift in the total area. Statistical plots of bedding dips based on 85 readings are presented in Figure. 6, indicating a structural average dip of 30 degrees N25E and strike N65W-S65E (Fig. 10).

Drawing cross section use the dip bedding
 StrucView automatic models utilize measured dips to visualize sedimentary structures. StrucView is ideal for enhanced cross-section modeling for several reasons:

1. Delineating tectonic structures from dips
2. Automatic Schmidt Analysis to determine axial plane of the structures
3. Modeling the structures in the vicinity of well No.
4. Cross-section is generated from the dip sticks and axial plane (similar to the fold model or parallel fold model)
5. It is a rapid method (Schlumberger, 2005; Darling, 2005).

In the wells studied, the cross sections were drawn using all the dips, beddings and bed strike data, as well as maximum dip data. These sections are drawn using the StrucView software next to the lithology columns drawn by the Litho ToolKit software. Litho Tool Kit software operates based on the neural network and uses the logs that delineate the lithology column. In this study, the density log (RHOB), gamma ray log (GR), neutron log (NPHI) and photo-electric factor log (PEF) were defined for the software to determine the name and lithology patterns in the sections, while the relationships between the logs were used as an index for specific lithologies. Finally, after defining the lithology patterns, the lithology of the other parts in the interval was delineated (Figs. 11, 12).

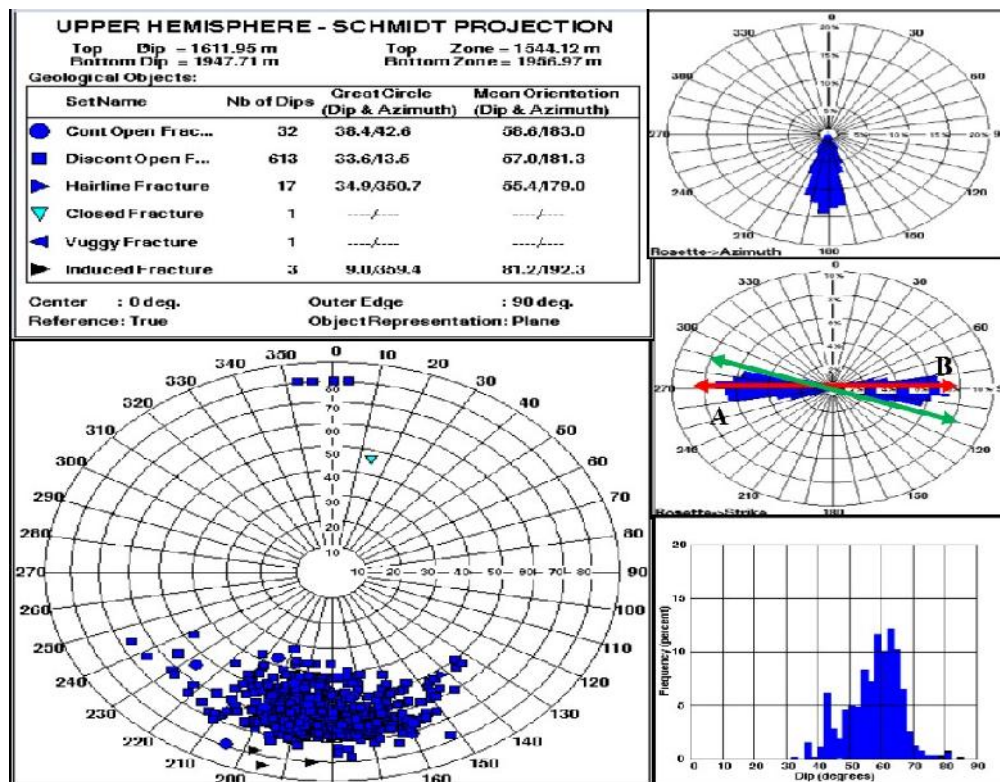


Figure 9. Stereonet, rose diagram and histogram of fractures in the well 3

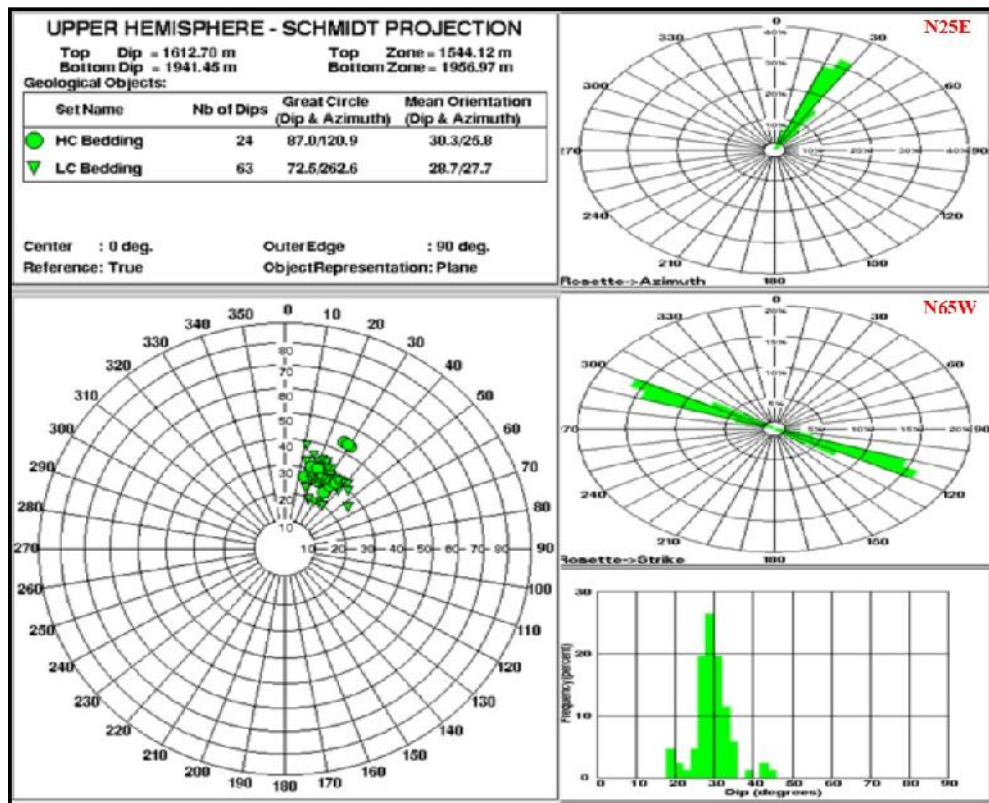


Figure 10. Stereonet, rose diagram and histogram of bedding in the well 3

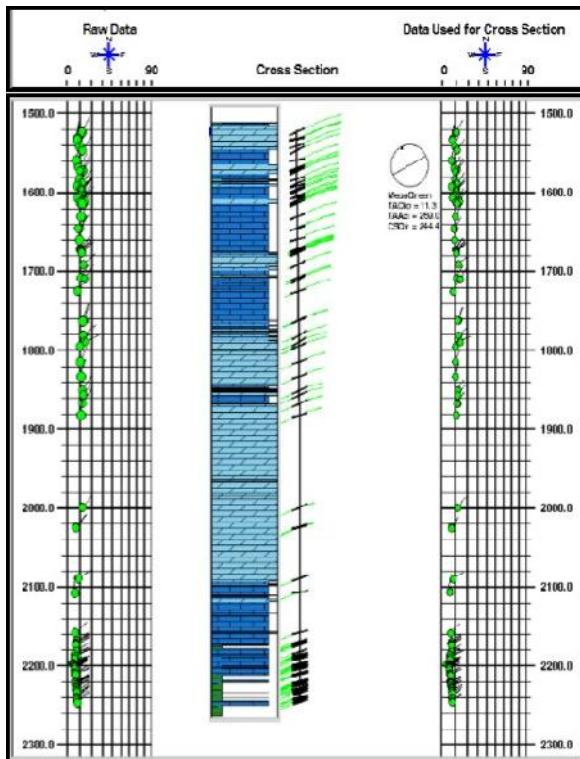


Figure 11. Cross section for well 6

Orientations of breakouts and induced fractures

For a well that is aligned with a principal stress axis, high compressive stresses are predicted in the direction of the least principal stress in the plane and perpendicular or tensile stresses in the direction of the greatest principal stress. These stress concentrations around the wellbore eventually lead to failure of the borehole wall. Two types of borehole failures are commonly used to determine the orientation of the principal stresses, viz., breakouts and induced fractures.

The identification and analysis of the borehole breakouts as a technique for *insitu* measurement of stress orientation and magnitude and identifying the orientation (azimuth) of both naturally occurring and induced fractures (hydrofractures), has received a great deal of attention over the past decade. Knowledge of the orientation of the horizontal earth stresses derived from an analysis of borehole breakouts is important in the study area mentioned. Borehole breakout typically appears on resistivity image logs as broad, parallel and poorly resolved conductive zones separated by 180° (i.e. observed on opposite sides of the borehole). Breakouts are typically conductive and

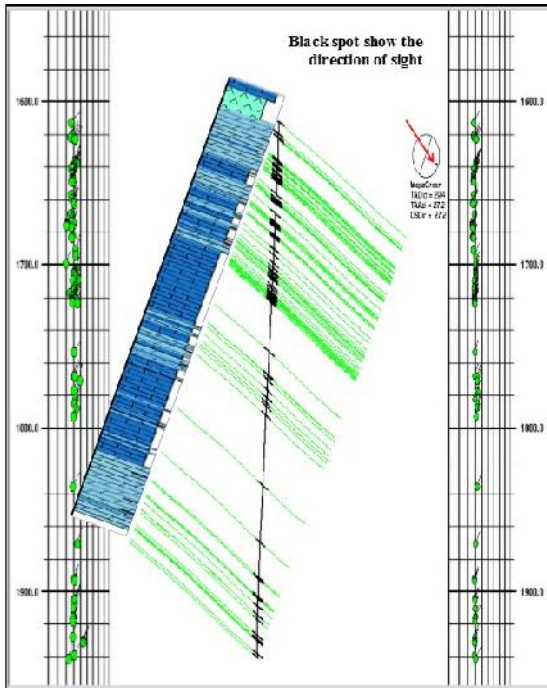


Figure 12. Cross section for well 3

poorly resolved because the wellbore fracturing and spalling associated with them result in poor contact between the tool pads and the wellbore wall, which in turn causes the tool to partially or fully measure the resistivity of the electrically conductive drilling mud, rather than the formation. Drilling- Induced Fractures (DIFs) typically develop as narrow sharply defined features that are sub-parallel or slightly inclined to the borehole axis in vertical wells and are generally not associated with significant borehole enlargements in the fracture direction. The stress concentration around a vertical borehole is at a minimum in the SH direction. Hence, DIFs develop approximately parallel to the SH orientation. Drilling-induced fractures can only be observed on the image logs. DIFs typically become infiltrated by the drilling mud (Tingay *et al.*, 2005).

Schematic cross- section of a wellbore shows the orientation of breakouts and induced fractures relative to the borehole, perpendicular to the *in situ* earth stress components. In most parts of the world, one of three principal stresses is oriented vertically, which requires the other two to be oriented horizontally. However, inclined stress fields do occur, especially in tectonically active areas. Breakouts form in response to the minimum and maximum stress components that are oriented

perpendicular to the wellbore. Note that these components may or may not be the principal stresses depending on the orientation of the wellbore relative to the *in-situ* stress field. Induced fractures tend to form perpendicular to the least principal stress, so that well-developed, borehole-parallel induced fractures form when σ_3 is oriented perpendicular to the borehole (Fig. 14) (Tingay *et al.*, 2008).

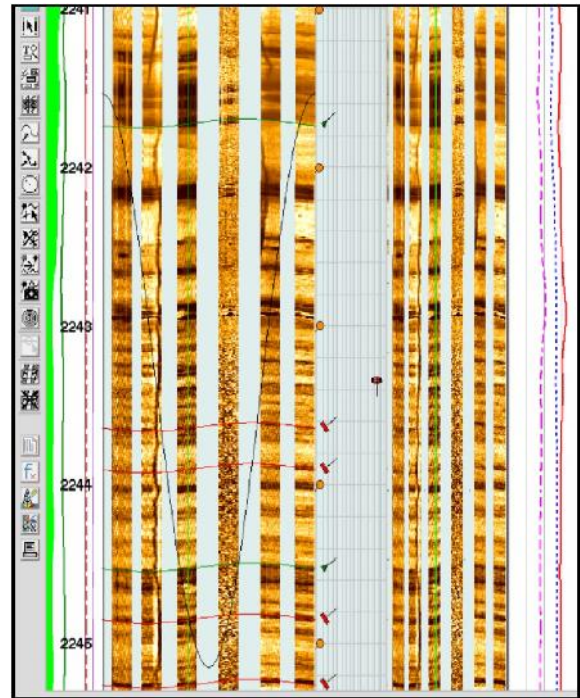


Figure 13. Example of Induce fracture on EMI in the well 6, subzone 2-3

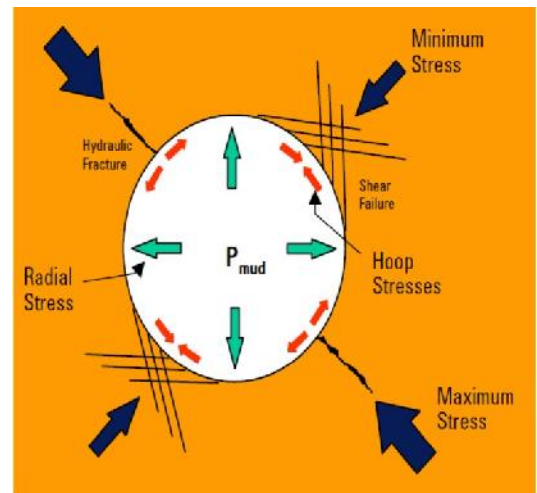


Figure 14. Schematic cross-sections of borehole breakout and drilling-induced fracture (Schlumberger, 2003)

Hydraulic induced fractures tend to be inclined to the wellbore when 3 are inclined to the wellbore, although in this case, they may not be formed perpendicular to 3. Its trend is an indication of the minimum horizontal. *In situ* stress

orientations were determined based on borehole breakouts identified in well No. 6. The EMI images showed borehole breakout striking on the average NW-SE (Fig. 15A), which is parallel to the minimum horizontal stress orientation in this area.

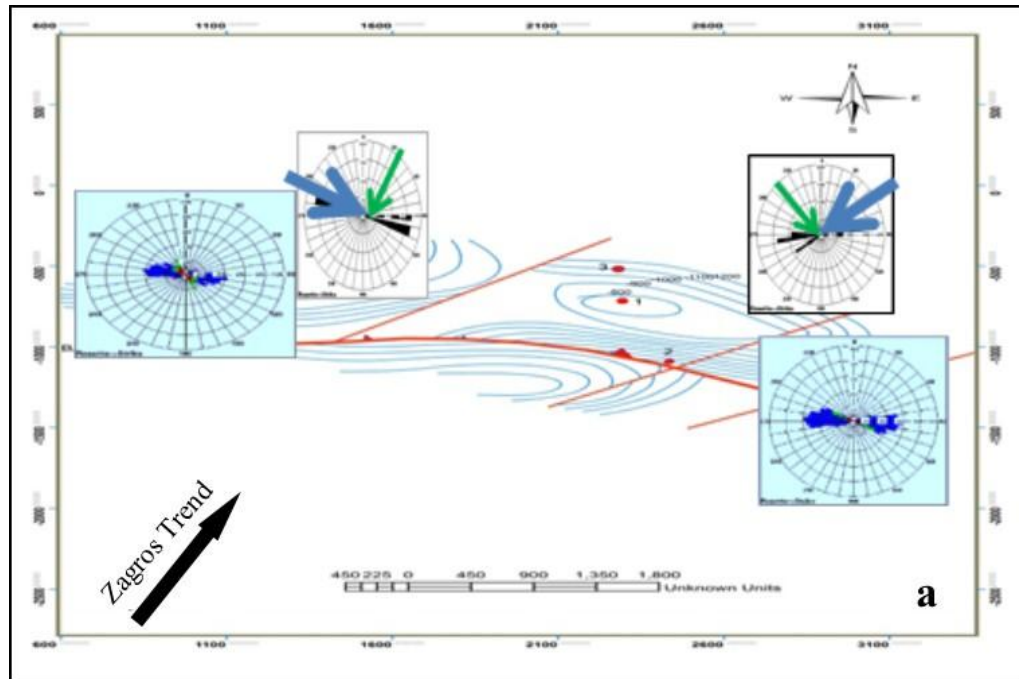


Figure 15 a. Maximum and minimum main stresses direction in the field around wells (blue arrows indicate max stress and green arrows indicate min stress) using the induced fractures. Stress directions different from western section. Therefore, western section does not follow Zagros trend to have Balarud shear zone

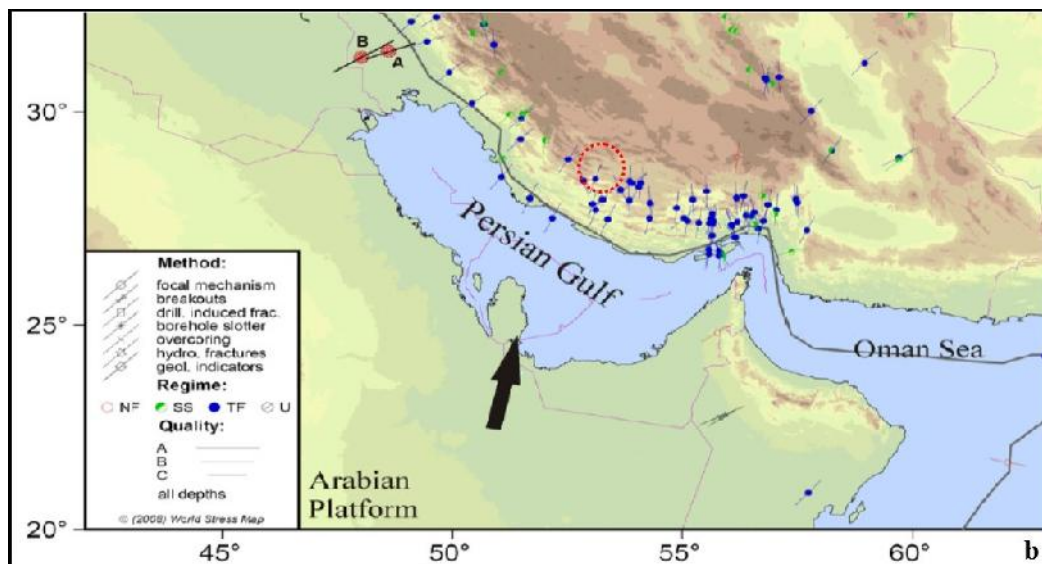


Figure 15 b. Maximum horizontal stress orientations in Iran from the World Stress Map database and from the wells analyzed herein. Red circle shows location of studied wells and heavy arrow shows motion of the Arabian plate relative to the Eurasia (Rajabi *et al.*, 2010)

Any drill induced on this well and well No. 3 in the maximum horizontal stress direction, therefore, can be inferred to be NW-SE. If they had developed, they would be oriented NE-SW, to be parallel to the maximum horizontal stress orientation. In this oil field, stress direction is different in the Eastern section compared with the Western one.

Therefore, the western section does not follow the general Zagros Trend (Alavi, 2004, 2007) to have the Balarud shear zone (Fig. 15B). Maximum horizontal stress direction in the eastern section, therefore, can be inferred to be NE-SW by the EMI in well No. 6 and FMI in well No. 2 (Fig. 15). It should be noted that the wrong determination of the *insitu* stress direction may cause borehole collapse so the perforating process needs to be done in the direction of maximum stress (Mohebbi *et al.*, 2007).

Conclusions

1. EMI has special characteristics that differentiate it from other tools. For example, one of the important EMI features is that it utilizes six articulating pads, each mounted on an independent arm, facilitating improved electrode-to-formation contact. The superior imaging is produced through consistent pad contact with the borehole wall which provides accurate, sharp images. Another important ability of the EMI is the great depth of investigation, almost 20 times more than that of the FMI tool. This capability is vital for the study of the vuggy reservoirs measuring their density and their connectivity. The EMI cuts costs by reducing coring intervals and accurately determining the perforation zones.

2. The well No. 3 statistical plots of bedding dips based on 85 readings indicated a structural average dip of 30 degrees N25E and strike of N65W-S65E. In this well, the axis re-circulation is the cause of the bedding shift than the total area and in well No. 6 the structural dip is deduced to be 8 degrees toward S60E and strike N30W. As this well is far away from the strike-slip and Balarud fault, beddings are more regular and their dips are less than those observed in other wells.

3. Fracture type can be classified as those fractures related to foldings that are based on relative fractures strike and bedding strike. These fractures are classified into two groups: oblique and longitudinal sets. In well No. 3, the longitudinal set

has the same strike as the bedding (N80W) and the oblique set strikes are N70E. In this well 665 open fractures are present. Their dip inclination varies from 30 to 80° and their strike is dominantly N-E while their azimuth varies from 180 to 200° from the north. In well No. 6 there are 485 open/closed fractures, their dip inclination varies from 30 to 60 degrees and their strike are dominantly N80W while their azimuth varies from 190 to 200° from the north. The longitudinal set strike in this well is N80W and the oblique set strike is N75E.

4. In this oil field, borehole breakout and induced fractures show stress direction very different from those of the western section. Therefore, the western section does not follow the Zagros trend to include the Balarud shear zone. In the western section, the maximum horizontal stress direction, therefore, can be inferred to be N75W-S75E to N15W-S15W by FMI on well No. 3 and EMI in well No. 6. In the eastern section the maximum horizontal stress direction, therefore, can be inferred to be N50E-S50W by the EMI on well No. 6 and FMI on well No. 3 (Zagros trend).

5. StrucView and Litho Toolkit software results on the dips and lithology in the different zones had a large correlation with the petrophysical logs and graphic well logs results. Dominating the reservoir lithology is limestone, dolomitic limestone and shaly limestone with anhydrite veins. Fractures are concentrated in the limestone and dolomite zones.

6. This oil field is a fault-bend fold that has strictly been influenced by the Balarud shear zone. The existence of the Balarud reverse fault and three strike-slip faults at the southern edge has caused great difficulty in the structural analyses. For example, the high density fractures in well No. 3 are related to the Axis Re-circulation by strike-slip fault nearby.

7. Regarding the stresses they are reverse on the western section for the presence of the Balarud shear zone. This oil field is a new exploratory oil field and the right maximum stress should be considered in the future for drilling as well as the best method for drilling which is the deviation drilling for the high density fractures in the Asmari reservoir.

Acknowledgment

The authors thank the National Iranian South Oil Company (NISOC) for sponsorship, data preparation and permission to publish the data. The

authors extend their gratitude to S. Tabatabayifor his cooperation and also sincerely thank Bahman

Soleimani and Abbas Charchi for their insightful and constructive reviews.

References

- Aghli, G., 2013. Fracture analysis of Asmari reservoir in Balarud oil field using the image logs. Mc.S. thesis. Shahid Chamran University, Ahvaz, Iran, 166 pp.
- Ahmadhadi, F., Daniel, J., Azzizadeh, M., and Lacombe, O., 2007. Evidence for pre-folding vein development in the Oligo-Miocene Asmari Formation in the Central Zagros Fold Belt, Iran. *Tectonics*, 1–22.
- Alavi, M., 2004. Regional stratigraphy of the Zagros fold-thrust belt of Iran and its proforeland evolution. *American Journal of Science*, 304 (1): 1- 20.
- Alavi, M. (2007). Structures of the Zagros fold-thrust belt in Iran. *American Journal of Science*, 307 (9): 1064–1095.
- Anselmetti, F.S., Eberli G.P., 1999. The Velocity Deviation Log: A Tool to Predict Pore Type Permeability Trends in Carbonate Drill Holes From Sonics And Porosity or Density Logs, *AAPG Bulletin*, 83(3): 450-466
- Bell, J. S. (1996). Petro Geoscience 1. IN SITU STRESSES IN SEDIMENTARY ROCKS (PART 1): MEASUREMENT TECHNIQUES. *Geoscience Canada*; 23- 2
- Berberian, M., King, G.C.P., 1981. Towards a paleogeography and tectonic evolution of Iran, *Can. J. Earth Sci.* 18: 210–265.
- Darling, T., 2005. *Well Logging and Formation Evaluation* Elsevier Science. 336 p..
- DeMets, C., Gordon, R.G. Argus, D.F., 2010. Geologically current plate motions. *Geophys. J. Int.* 181: 1–80.
- Gholipour, A. M., 1998. Patterns and structural positions of productive fractures in the Asmari Reservoirs, Southwest Iran. *Journal of Canadian Petroleum Technology*, 37(1): 44- 50.
- Halliburton. 1996. *Electrical Micro Imaging Service (Sales Kit)*. 71 pp.
- Khoshbakht, F., Memarian, H., Mohammadnia, M., 2009. Comparison of Asmari, Pabdeh and Gurpi formation's fractures, derived from image log. *Journal of Petroleum Science and Engineering*, 67(1-2): 65–74.
- McQuillan, H. (1973). Small-scale fracture density in Asmari formation of southwest Iran and its relation to bed thickness and structural setting. *AAPG Bulletin*, 57: 2367–2385.
- McQuillan, H. 1974. Fracture patterns on Kuh-e Asmari Anticline, Southwest Iran. *AAPG Bulletin*, 58(2): 236- 246.
- Mohebbi, A., Haghighi, M., Sahimi, M. 2007. Conventional logs for fracture detection and characterization in one of the Iranian field. In *International Petroleum Technology Conference*, 4-6 December, Dubai, U.A.E. Dubai: International Petroleum Technology Conference.
- Rajabi, M., Sherkati, S., Bohloli, B., Tingay, M., 2010. Subsurface fracture analysis and determination of in-situ stress direction using FMI logs: An example from the Santonian carbonates (Ilam Formation) in the Abadan Plain, Iran. *Tectonophysics*, 492(1-4): 192- 200.
- Rezaee, M. R., Chahrazi, A. 2005. *Fundamentals of Well Log Interpretation (First Edit., p. 699)*. Tehran: University of Tehran (in Persian).
- Rezaie, A. H., Nogole-Sadat, M. A., 2004. Fracture Modeling in Asmari Reservoir of Rag-e Sefid Oil-Field by using Multiwell Image Log (FMS/FMI). *Iranian International Journal of Science*, 5(1): 107–121.
- Ricou, L.E., 1974. L'évolution géologique de la région de Neyriz (Zagros iranien) et l'évolution structurale des zagrides, Thèse. Université d'Orsay, France.
- Rider, H., 1996. *The Geological Interpretation of Well Logs*. Gulf Publishing.
- Roehl, P.O., Choquette, P. W. 1985. *Carbonate Petroleum Reservoirs*. Springer-Verlag. 622 pp.
- Saedi, G., 2010. Fracture analysis of Asmari reservoir in Lali oil field using the FMI image log. Mc.S. thesis. Shahid Chamran University, Ahvaz, Iran. 190 pp.
- Sahabi, F. 2010. Study of Balarud rivers fault and its roles on the area structural. 6th International Conference on Seismology and Earthquake Engineering. SEE6/ /IIEES, (In Persian).
- Sepher, M, Cosgrove, J, 2005. The role of the Kazerun Fault Zone in the formation and deformation of the Zagros Fold–Thrust Belt, Iran. *Tectonics*, 24
- Schlumberger (1994). *FMI Fullbore Formation MicroImager*. Houston: Schlumberger Educational Services.
- Schlumberger (2003). Using borehole imagery to reveal key reservoir features. In *Reservoir Optimization Conference*. Tehran, Iran.
- Schlumberger (2005). *GeoFrame 4.2, BorView User's Guide*. Schlumberger Ltd.
- Serra, O. (1989). *Formation MicroScanner image interpretation* (p. 117). Schlumberger Educational Services.
- Serra, O., Serra, L., 2004. *Well Logging: Data Acquisition and Applications* (p. 674). Editions Technip. Retrieved from
- Stocklin, J., (1968). Structural history and tectonics of Iran: a review. *AAPG Bull.* 52: 1229- 1258.
- Tingay, M., Müller, B., Reinecker, J., Heidbach, O., Wenzel, F., & Fleckenstein, P., 2005. Understanding tectonic stress in the oil patch; the World Stress Map Project. *Leading Edge*, 24(12): 1276- 1282.

- Tingay, M., Reinecker, J., Müller, B., 2008. Borehole breakout and drilling-induced fracture analysis from image logs. World Stress Map Project.
- Tokhmechi, B. (2009). Identification and categorization of joints using data fusion approach, emphasizing on Asmari Formation. University of Tehran. 155pp.
- Ye, S., Rabiller, P., 1998. Automated fracture detection on high resolution resistivity borehole imagery. In SPE annual technical conference and exhibition 777–784 pp.